



ORIGINAL ARTICLE

# A performance-oriented power transformer design methodology using multi-objective evolutionary optimization



Amr A. Adly <sup>a,\*</sup>, Salwa K. Abd-El-Hafiz <sup>b</sup>

<sup>a</sup> *Electrical Power and Machines Department, Faculty of Engineering, Cairo University, Giza 12613, Egypt*

<sup>b</sup> *Engineering Mathematics Department, Faculty of Engineering, Cairo University, Giza 12613, Egypt*

## ARTICLE INFO

### Article history:

Received 26 May 2014

Received in revised form 8 August 2014

Accepted 10 August 2014

Available online 20 August 2014

### Keywords:

Power transformers

Design

Multi-objective evolutionary optimization

Particle swarm optimization

## ABSTRACT

Transformers are regarded as crucial components in power systems. Due to market globalization, power transformer manufacturers are facing an increasingly competitive environment that mandates the adoption of design strategies yielding better performance at lower costs. In this paper, a power transformer design methodology using multi-objective evolutionary optimization is proposed. Using this methodology, which is tailored to be target performance design-oriented, quick rough estimation of transformer design specifics may be inferred. Testing of the suggested approach revealed significant qualitative and quantitative match with measured design and performance values. Details of the proposed methodology as well as sample design results are reported in the paper.

© 2014 Production and hosting by Elsevier B.V. on behalf of Cairo University.

## Introduction

It is well known that transformers are regarded as indispensable and crucial components in power systems. Due to market globalization, and in some cases to accommodate particular specification requests, transformer manufacturers are facing an increasingly competitive environment to maintain their

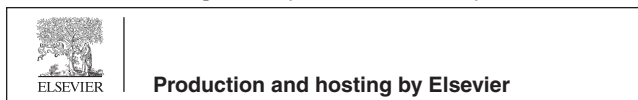
sales figures. This competitive environment mandates the adoption of design strategies yielding better performance at lower costs.

In the past, several power transformer design methodologies have been proposed [1–8]. Adly and Abd-El-Hafiz [1] demonstrated that feed-forward neural networks may be utilized to predict design details of power transformers after being trained using dimensional and winding details of a set of actual transformers. Alternatively, finite element analysis (FEA) coupled to an educated trial and error approach was introduced [2,3]. Furthermore, a computer-aided trial search looping algorithm aiming at minimizing transformer design cost has been demonstrated [4]. Other approaches coupling FEA to a knowledge-based design optimization strategy and genetic algorithms were presented [5–7]. Hernández and Arjona [8] proposed

\* Corresponding author. Tel.: +20 100 7822762; fax: +20 2 35723486.

E-mail address: [adlyamr@gmail.com](mailto:adlyamr@gmail.com) (A.A. Adly).

Peer review under responsibility of Cairo University.



another approach that couples classical design equations to an intelligent design search algorithm.

A quick review of these methodologies reveals that a wide span of design strategies could be utilized to achieve an optimum power transformer design. For instance, analytical formulations may be utilized for the quick estimation of transformer dimensions and design details. Methodologies based upon more accurate FEA computations offer precise estimation of transformer performance measures, provided that design specifics are suggested a priori. Other methodologies, on the other hand, may utilize a hybrid strategy or even non-traditional heuristic and/or evolutionary computation approaches.

Several techniques have addressed transformer design problems using single-objective Particle Swarm Optimization (PSO). Hengsi et al. [9] demonstrated that the two objectives of minimizing power loss and leakage inductance were combined into one objective function using weighted aggregation. Single-objective evolutionary optimization was, then applied using a hybrid algorithm of PSO and differential evolution. Rashtchi et al. [10] and Jalilvand and Bagheri [11] also utilized single-objective PSO in the optimal design of protective current transformers. The objectives of making current measurements more accurate and designing more efficient current transformers in terms of both size and cost were formulated as an optimization problem to be solved by PSO. On the other hand, Du et al. [12,13] focused on improving the standard single-objective PSO algorithm and utilizing the improved version in the optimal design of rectifier transformers. The purpose of the improvement was to avoid being trapped in local optima.

The reduction of a multi-objective optimization problem to a single-objective problem is usually performed by constructing a weighted sum of the original objective functions. While such methods are easy to implement and use, it is difficult to determine the appropriate weight coefficients when enough information about the problem is not available. Another drawback of such approaches is that several runs of the algorithm are needed in order to obtain a set of optimal compromise solutions to choose from. Furthermore, some optimal solutions cannot be obtained, in some cases, regardless of the weight combinations used [14]. Hence, multi-objective PSO becomes useful as it enables finding several optimal compromise solutions in a single run of the algorithm instead of having to perform a series of separate runs as in the case of classical optimization methods.

The purpose of this paper is to present a power transformer design methodology using multi-objective evolutionary optimization. Using this methodology, which is tailored to be target performance design-oriented, quick rough estimation of transformer design specifics may be inferred. Estimated design parameters and details using the proposed methodology may also be considered for further refinement by other FEA approaches. It should be stated that while the proposed methodology is analytical in nature, some parameter range settings have utilized previously reported power transformer field computation results. Details of the proposed methodology as well as sample design results are reported in the following sections.

### Performance-oriented power transformer design approach

In addition to the mandated primary line voltage  $V_{l1}$ , secondary line voltage  $V_{l2}$  and supply frequency  $f$ , a three-phase

power transformer design is usually optimized to meet volt-ampere rating  $S$ , total copper losses  $P_{cu}$ , no-load losses  $P_{NL}$  and equivalent reactance  $X$  requirements. In other words, a performance-oriented design problem reduces to the proper selection of windings and dimensional details that would lead to a set of targeted performance figures. Expressions linking the above-mentioned performance figures to the windings and dimensional details of a three-phase power transformer may be deduced in a systematic way as given below (please refer, for instance, to [15–17]).

$$\frac{V_{l1}}{\sqrt{3}} = 4.44fBK_fK_c \frac{\pi}{4} D^2 N_1, \quad (1)$$

where  $B$  is the core maximum flux density (magnetic loading),  $K_f$  is the laminations stack factor,  $K_c$  is the gross area to maximum circular area ratio,  $D$  is the core bounding diameter and  $N_1$  is the primary winding number of turns.

It is also known that the window space factor of a three-phase transformer  $S_W$  may be expressed as:

$$S_W = \frac{2N_1a_{c1} + 2N_2a_{c2}}{H_W W_W}, \quad (2)$$

where  $N_2$  is the secondary winding number of turns,  $H_W$  is the window height,  $W_W$  is the window width, while  $a_{c1}$  and  $a_{c2}$  represent the primary and secondary winding cross sectional areas, respectively.

Denoting the window height to width ratio by  $K_W$  and assuming a common current density (electric loading)  $J$  in both windings while  $N_1 I_{ph1} = N_2 I_{ph2}$  (where  $I_{ph1}$  and  $I_{ph2}$  are the primary and secondary phase currents), expression (2) may be rewritten in the form:

$$S_W = \frac{4N_1a_{c1}K_W}{H_W^2}. \quad (3)$$

It should be pointed out here that, usually, current densities in low and high voltage windings are not identical due to standard wire size availability and/or other design factor constraints. Nevertheless, the assumed current density  $J$  may be regarded as an average figure for both windings.

From expressions (1) and (3), the volt-ampere rating of a three-phase transformer may thus be expressed as:

$$S = 3 \left\{ 4.44fBK_fK_c \frac{\pi}{4} D^2 N_1 \right\} \left\{ J \frac{S_W H_W^2}{4K_W N_1} \right\} \\ = \left( \frac{3.33\pi K_f K_c S_W f}{4K_W} \right) J B D^2 H_W^2. \quad (4)$$

Total copper losses  $P_{cu}$  may actually be regarded as a superposition of three components. Namely, these three components are the ohmic winding losses  $P_{cu-ohmic}$ , the eddy current losses in the windings  $P_{cu-eddy}$  and the copper terminals connection losses  $P_{cu-con}$ . While designing a transformer to meet pre-mandated specification, maintaining the total copper losses below the threshold values becomes a must. In order to achieve this goal, accurate time consuming computations have to be carried out. Alternatively, appropriate computational safety factors may be applied to fast analytical design methodologies.

While  $P_{cu-con} \leq 0.05P_{cu-ohmic}$ , eddy current losses in transformer windings are dependent on the window height to width ratio  $K_W$ . As previously reported by Saleh et al. [18], electromagnetic field computation results suggest that, taking  $2 \leq K_W \leq 2.5$ , winding eddy current losses may be estimated as  $P_{cu-eddy} \leq 0.15P_{cu-ohmic}$ .

From the previous common electric loading assumptions and for the aforementioned  $K_W$  range, total copper losses may thus be given by the expression:

$$P_{cu} \approx 1.2 \left( \frac{3I_{ph1}^2 \rho_{cu} N_1 l_{m1}}{a_{c1}} + \frac{3I_{ph2}^2 \rho_{cu} N_2 l_{m2}}{a_{c2}} \right) \\ = 7.2J^2 \rho_{cu} N_1 a_{c1} l_{m1} = 1.2J^2 \rho_{cu} Vol_{cu}, \quad (5)$$

where  $\rho_{cu}$  is the specific resistivity of copper,  $Vol_{cu}$  is the overall copper volume, while  $l_{m1}$ ,  $l_{m2}$  and  $l_{m1}$  represent the average turn length of the primary, secondary and both windings, respectively.

No-load losses  $P_{NL}$ , on the other hand, may also be regarded as a superposition of two components. More specifically, these two components are the core losses  $P_{Fe}$  and stray losses  $P_{stray}$ . Once more, it should be stated that accurate estimation of the stray losses requires massive computational resources that involve complex models of coupled magnetic, thermal and mechanical variables (please refer, for instance, to [19–21]). By adopting standard fabrication methodologies [15–17], stray losses may be estimated in accordance with the inequality  $P_{stray} \leq 0.3P_{Fe}$ . Consequently, an upper limit for the no-load losses may be expressed in the form:

$$P_{NL} \approx 1.3P_{Fe} = 1.3W_{Fe}(B, f) \delta_{Fe} Vol_{Fe} \\ \approx 1.3W_{Fe}(B, f) \delta_{Fe} \left( K_f K_c \frac{\pi}{4} D^2 \right) (3H_W + 4W_W + 6D) \\ \approx 1.3W_{Fe}(B, f) \delta_{Fe} K_f K_c \frac{\pi}{4} D^2 \left[ \left( \frac{3K_W + 4}{K_W} \right) H_W + 6D \right], \quad (6)$$

where  $\delta_{Fe}$  is the steel lamination density and  $W_{Fe}(B, f)$  is the specific core losses as a function of flux density and frequency that may be deduced by referring to the core lamination specifications data sheet. Please note that explicit function formulation for  $W_{Fe}(B, f)$  is either given in manufacturers' specification sheets or simply inferred by fitting reported curves.

Referring to [15], the equivalent transformer reactance may be computed from:

$$X = 2\pi f \mu_o N_1^2 \frac{l_{m1}}{l_{WH}} \left( a + \frac{b_1 + b_2}{3} \right), \quad (7)$$

where  $\mu_o$  is the permeability of free space,  $l_{WH}$  is the windings height,  $a$  is the spacing between the low and high voltage windings, while  $b_1$  and  $b_2$  represent the gross primary and secondary winding thicknesses, respectively. Following the assumption of

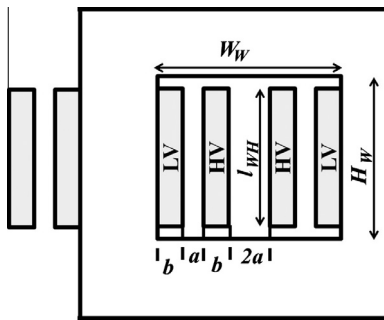


**Fig. 1** Assumed winding configuration within the transformer window dimensions.

identical current densities for both windings and assuming similar winding heights, winding thicknesses may be assumed equal such that  $b_1 = b_2 = b$  (please refer to Fig. 1).

Usually, the spacing between high voltage (outer) windings is double the distance between a low voltage (inner) winding and its corresponding high voltage winding. In other words, the total window width  $W_W$  may be approximated by  $W_W \approx 4(a + b)$ . From practical industrial considerations  $a \approx b/4$ . In this case, the winding thickness may be correlated to the window dimensions according to:

$$b \approx \frac{W_W}{5} \approx \frac{H_W}{5K_W}. \quad (8)$$

Denoting the winding height  $l_{WH}$  to the window height  $H_W$  ratio by  $K_H$  and following the previously stated practical assumptions as well as (8), expression (7) may be rewritten in the form:

$$X = 2\pi f \mu_o N_1^2 \frac{\pi(D + 2b + a)}{K_H H_W} \left( a + \frac{2b}{3} \right) \\ = \frac{11\pi^2 f \mu_o N_1^2}{30K_H K_W} \left( D + \frac{9H_W}{20K_W} \right). \quad (9)$$

From (3),  $N_1$  may be expressed in the form:

$$N_1 = \frac{S_W H_W^2}{4K_W a_{c1}} = \frac{S_W H_W^2 J}{4K_W I_{ph1}}. \quad (10)$$

Substituting (10) into (9), we obtain:

$$X = \frac{11\pi^2 f \mu_o S_W^2}{480K_H K_W^3 I_{ph1}^2} J^2 H_W^4 \left( D + \frac{9H_W}{20K_W} \right). \quad (11)$$

Following the same window configuration assumptions, expression (5) may be rewritten in the form:

$$P_{cu} \approx 7.2J^2 \rho_{cu} \frac{S_W H_W^2}{4K_W} \pi \left( D + \frac{9H_W}{20K_W} \right) \\ = \frac{7.2\pi \rho_{cu} S_W}{4K_W} J^2 H_W^2 \left( D + \frac{9H_W}{20K_W} \right). \quad (12)$$

By referring to Eqs. (4), (6), (11) and (12), it is clear that the target performance oriented three-phase transformer design problem may be reduced to the proper selection of four unknowns. Namely, those unknowns are the current density  $J$ , the maximum core magnetic flux density  $B$ , the transformer core diameter  $D$ , and the window height  $H_W$ .

Dividing (11) by (12), we get:

$$\frac{X}{P_{cu}} = \frac{11\pi f \mu_o S_W}{864\rho_{cu} K_H K_W^2 I_{ph1}^2} H_W^2. \quad (13)$$

Consequently,  $H_W$  may be deduced from the expression:

$$H_W = \sqrt{\frac{864\rho_{cu} K_H K_W^2 I_{ph1}^2}{11\pi f \mu_o S_W} \frac{X}{P_{cu}}}. \quad (14)$$

After obtaining  $H_W$  value, remaining unknowns may be deduced by solving (4), (6) and (12). Given the highly nonlinear nature of the equations under consideration, multi-objective optimization is needed to achieve a minimum cost design subject to the range restrictions for unknowns  $J$ ,  $B$  and  $D$ . Details of the multi-objective problem formulation are given in the following section.

### Formulation as a multi-objective optimization problem

In engineering design problems, computational models are often used to describe the complex behaviors of physical systems and optimal solutions are sought with respect to some performance criteria. Hence, multi-objective optimization becomes useful in obtaining a set of optimal compromise solutions (Pareto-optimal front) so that the designer can select the best choice.

The basic concepts of multi-objective optimization are introduced using a  $d$ -dimensional search space,  $\mathcal{S} \subset \mathcal{R}^d$ , and  $k$  objective functions defined over  $\mathcal{S}$  as given by Bui and Alam [22]:

$$f(x) = [f_1(x), f_2(x), \dots, f_k(x)], \quad (15)$$

subject to  $m$  inequality constraints:

$$g_i(x) \leq 0, \quad i = 1, \dots, m. \quad (16)$$

The aim was to find a solution,  $x^* = (x_1^*, x_2^*, \dots, x_d^*)$ , that minimizes  $f(x)$ . The objective functions  $f_i(x)$  may be conflicting with each other, thereby preventing the detection of a single global minimum at the same point in  $\mathcal{S}$ . Consequently, optimality of a solution in multi-objective problems is defined differently.

A vector  $v = (v_1, v_2, \dots, v_k)$  is said to dominate a vector  $u = (u_1, u_2, \dots, u_k)$  for a multi-objective minimization problem if and only if  $v_i \leq u_i$  for all  $i = 1, 2, \dots, k$  and  $v_i < u_i$  for at least one component, where  $k$  is the dimension of the objective space. A solution  $u \in U$ , where  $U$  is the universe, is said to be Pareto optimal if and only if there exists no other solution  $v \in U$ , such that  $u$  is dominated by  $v$ . Such solutions,  $u$ , are called non-dominated solutions. The set of all such non-dominated solutions constitutes the Pareto-optimal front.

For the transformer design approach under consideration,  $S$ ,  $P_{cu}$ ,  $P_{NL}$  and  $X$  are given as target performance requirements. The window height  $H_W$  is first calculated from expression (14). Multi-objective optimization is then utilized to determine the other leading design parameters;  $J$ ,  $B$  and  $D$ . Hence,  $x^* = (J, B, D)$ . Within the current implementation, expressions (15) and (16) are formulated as:

$$f(x) = \left[ \left( \frac{S^{cmp}(x^*) - S}{2} \right)^4, (P_{cu}^{cmp}(x^*) - P_{cu})^4, \left( \frac{P_{NL}^{cmp}(x^*) - P_{NL}}{4} \right)^4 \right], \quad (17)$$

subject to the following  $x^*$  inequality constraints:

$$\begin{bmatrix} J_l \\ B_l \\ D_l \end{bmatrix} \leq \begin{bmatrix} J \\ B \\ D \end{bmatrix} \leq \begin{bmatrix} J_u \\ B_u \\ D_u \end{bmatrix}, \quad (18)$$

where  $S^{cmp}$ ,  $P_{cu}^{cmp}$  and  $P_{NL}^{cmp}$  are the computed volt-ampere rating, the computed total copper losses and the computed no-load losses, respectively. It should be pointed out that the inequality ranges given in (18) should be in accordance with the typical lower and upper limits of  $J$ ,  $B$  and  $D$  for power transformers in the range under consideration.

### Multi-objective particle swarm optimization

Inspired by the behavior of bird flocks or insect swarms, Kennedy and Eberhart first proposed PSO in 1995 [23]. PSO is a

population based heuristic, where the population of the potential solutions is called a swarm and each individual solution within the swarm is called a particle. Considering a  $d$ -dimensional search space, an  $i$ th particle is associated with a position in the search space  $x_i = (x_{i,1}, \dots, x_{i,d})$ , a velocity  $v_i = (v_{i,1}, \dots, v_{i,d})$  and an individual experience vector  $Pb_i = (Pb_{i,1}, \dots, Pb_{i,d})$  storing the position corresponding to the particle's personal best performance. Experience of the whole swarm is captured in the vector  $Gb = (Gb_1, \dots, Gb_d)$ , which corresponds to the position of the global best performance in the swarm.

The movement of a particle toward the optimum solution is governed by updating its velocity and position according to Eqs. (i) and (ii) shown in Fig. 2, respectively. While the parameter  $w$  is the inertia weight, parameters  $c_1$  and  $c_2$  are acceleration coefficients. Parameters  $r_1$  and  $r_2$  are random numbers, generated uniformly in the interval  $[0, 1]$  and are responsible for providing randomness to the flight of the swarm. The second term in Eq. (i) of Fig. 2 is the cognition term, which takes into account only the particle's individual experience. The third term in Eq. (i) of Fig. 2 is the social term, which signifies the interaction between the particles. The values of  $c_1$  and  $c_2$  allow the particle to tune the cognition and social terms, respectively. A larger value of  $c_1$  allows exploration, while a larger value of  $c_2$  encourages exploitation. Single objective PSO has been successfully utilized in many engineering applications such as the optimization of devices and systems [24,25] and field computation in nonlinear magnetic media [20,26,27].

In order to handle multi-objective optimization, several approaches adapt single objective PSO using the Pareto dominance concept to determine the best positions that will guide the swarm during search [22]. Additional criteria are also imposed to take into consideration further issues such as swarm diversity and Pareto front spread. In this paper, the Time Variant Multi-Objective Particle Swarm Optimization (TV-MOPSO) algorithm is utilized [28]. To achieve good balance between exploration and exploitation of the search space, TV-MOPSO is adaptive in nature with respect to its inertia weight and acceleration coefficients. A mutation operator is incorporated to resolve the problem of premature convergence

#### Algorithm TV-MOPSO

$M_s$ : size of the swarm,  $M_a$ : maximum size of the archive,  $M$ : maximum number of iterations,  $d$ : dimension of the search space,  $O_f$ : final output

##### (1) Initialize

- Randomly generate a swarm,  $Swrm_0$ .
- Initialize an archive  $A$ .

##### (2) For $t = 1$ to $M$

###### (2.1) For $i = 1$ to $M_s$ update the swarm, $Swrm_t$

###### (2.1.1) Update the velocity of each particle:

- Find the global best solution,  $Gb_t$ , from the archive.
- Find the personal best solution,  $Pb_i$ .
- Adjust the time variant parameters
- $v_{ij} = w v_{ij} + c_1 r_1 (Pb_{ij} - x_{ij}) + c_2 r_2 (Gb_j - x_{ij}) \quad \forall j \in \{1, \dots, d\}$  (i)

###### (2.1.2) Update the coordinates of each particle:

- $x_{ij} = x_{ij} + v_{ij} \quad \forall j \in \{1, \dots, d\}$  (ii)

###### (2.2) Update the archive, $A_t$

###### (2.3) Mutate the swarm, $Swrm_t$

##### (3) Return the Pareto optimal front, $O_f = A_t$

Fig. 2 Time variant multi-objective particle swarm optimization algorithm [22].

to the local Pareto-optimal front that is often observed in multi-objective PSO. An archive is also maintained to store the non-dominated solutions found during execution. The global best solution is selected from this archive using a diversity consideration.

Fig. 2 shows the TV-MOPSO algorithm, which consists of three main steps. The first step generates an initial swarm  $S_{wrm_o}$  of size  $M_s$  with zero velocities and random values for the coordinates from the respective domains of each dimension. An archive of maximum size  $M_a$  is initialized to contain the non-dominated solutions from  $S_{wrm_o}$ . The second step represents the main iteration cycle in which the swarm is updated, the archive is updated and the swarm is mutated at each iteration  $t$ .

The swarm  $S_{wrm_t}$  is updated, in step (2.1) of the algorithm, by updating the velocity and coordinates of each particle using Eqs. (i) and (ii) of Fig. 2, respectively. To update the velocity, the global best solution is obtained from the archive using a diversity consideration. The method for computing diversity of the solutions is based on a nearest neighbor concept [28]. The present solution is compared with the personal best solution, and replaces the latter only if it dominates that solution. Moreover, time variant parameters are adjusted [28]. These parameters include an inertia coefficient,  $w$ , a local acceleration coefficient,  $c_1$ , and a global acceleration coefficient,  $c_2$ .

The inertia coefficient  $w$  is decreased linearly with each iteration from an initial value  $w_i$  to a final value  $w_f$ . The value of  $w$  at iteration number  $t$  is calculated as:

$$w = (w_i - w_f) \times \frac{(M - t)}{M} + w_f, \quad (19)$$

where  $M$  is the maximum number of iterations.

To compromise between exploration and exploitation of the search space, the cognitive acceleration coefficient  $c_1$  and the social acceleration coefficient  $c_2$  are varied linearly with each iteration as given by (20) and (21), respectively. While  $c_1$  decreases from the initial value  $c_{1i}$  to the final value  $c_{1f}$ ,  $c_2$  increases from  $c_{2i}$  to  $c_{2f}$ .

$$c_1 = (c_{1f} - c_{1i}) \times \frac{t}{M} + c_{1i}, \quad (20)$$

$$c_2 = (c_{2f} - c_{2i}) \times \frac{t}{M} + c_{2i}. \quad (21)$$

The archive  $A_t$  is updated, in step (2.2) of the algorithm, by including the non-dominated solutions from the combined population of the swarm and the archive. If the size of the archive exceeds the maximum limit ( $M_a$ ), it is truncated using the diversity consideration [28].

To explore the search space to a greater extent, while obtaining better diversity, a mutation operator is used in step (2.3) of the algorithm shown in Fig. 2. Mutation is performed with probability inversely proportional to the chromosome length  $d$ . Given a particle  $p$ , a randomly chosen coordinate (i.e., variable) of the particle,  $p_k$ , is mutated as follows:

$$p'_k = \begin{cases} p_k + \Delta(t, p_{ku} - p_k) & \text{if flip} = 0 \\ p_k - \Delta(t, p_k - p_{kl}) & \text{if flip} = 1 \end{cases}, \quad (22)$$

where  $flip$ ,  $p_{kl}$  and  $p_{ku}$  denote the random event of returning 0 or 1, the lower and the upper limits of  $p_k$ . The function  $\Delta$  is defined by:

$$\Delta(t, x) = x \times \left(1 - r^{(1 - \frac{t}{M})^q}\right), \quad (23)$$

where  $r$  is a random number in the range  $[0, 1]$ ,  $M$  is the maximum number of iterations and  $t$  is the iteration number. The parameter  $q$  determines the mutation's dependence level on the iteration number.

After executing the specified number of iterations, the third and final step of the algorithm returns the final archive. This archive contains the final non-dominated front (i.e., Pareto optimal front).

## Implementation and design examples

To serve the testing and estimation purposes, the proposed design approach has been implemented in digital form. The methodology has been particularly utilized to design 25–50 MVA, 66 kV/11 kV, DYn11, 50 Hz power transformers subject to a variety of design performance constraints. As per practical transformer stacking and assembly measures for the MVA range under consideration, it was decided to set throughout the computations  $S_W = 0.2$ ,  $K_H = 0.9$ ,  $K_f = 0.95$ , and consider 11-step cores (leading to  $K_c = 0.958$ ) [15–17]. Common values for  $\mu_o$ ,  $\rho_{cu}$  and  $\delta_{Fe}$  were taken as  $4\pi \times 10^{-7}$  H/m,  $2.1 \times 10^{-8}$   $\Omega$  m and  $7.65 \times 10^3$  kg/m<sup>3</sup>, respectively. Using Armco Steel TRAN-COR-H0 CARLITE-3 core laminations, an expression for  $W_{Fe}(B, 50 \text{ Hz})$  was inferred from data offered by the manufacturer (please refer to [29]). The typical values of  $J_b$ ,  $J_u$ ,  $B_b$ ,  $B_u$ ,  $D_l$  and  $D_u$  for power transformers in the range under consideration are set as  $1.1 \times 10^6$ ,  $3.2 \times 10^6$ , 1.0, 1.8, 0.1, 0.7, respectively.

In order to test the proposed performance-oriented design methodology, two transformers (rated 25 MVA and 40 MVA) of known manufacturer design details and measured performances are considered. It should be stated here that a considerable number of units of these particular transformer designs, which obviously passed all standard routine tests, has been acquired and installed in several national and regional grid sub-stations. As previously discussed, measured performance figures of actual transformers are taken as the target design requirements for the design methodology.

The TV-MOPSO algorithm is executed using a swarm of  $M_s = 50$  particles, a maximum archive size of  $M_a = 200$  and for  $M = 1000$  iterations. The parameters used in the reported results are  $w_i = 0.7$ ,  $w_f = 0.4$ ,  $c_{1i} = 2.5$ ,  $c_{1f} = 0.5$ ,  $c_{2i} = 0.5$ ,  $c_{2f} = 2.5$  and  $q = 5$ . The Pareto front obtained for the 40 MVA transformer is shown in Fig. 3.

Out of a set of design parameters inferred by the TV-MOPSO implementation, the design corresponding to a minimum iron core volume is taken as the optimum choice. Comparisons between design parameters of the actual transformers and those proposed by the design methodology under consideration are given in Tables 1 and 2. Variations between actual and computed performance (as well as cost) figures are also given in the same tables. With the exception of the suggested current density  $J$ , it is clear that the proposed approach leads to good qualitative and quantitative performance-oriented design results. Moreover, the proposed higher  $J$  value by the suggested methodology may be regarded as a possible cost minimization option as indicated in Tables 1 and 2 by the possible reduction in the transformers copper volume.

Using the proposed approach, computations are also carried out to investigate the design parameters deviation from those of the 40 MVA test transformer as a result of changing

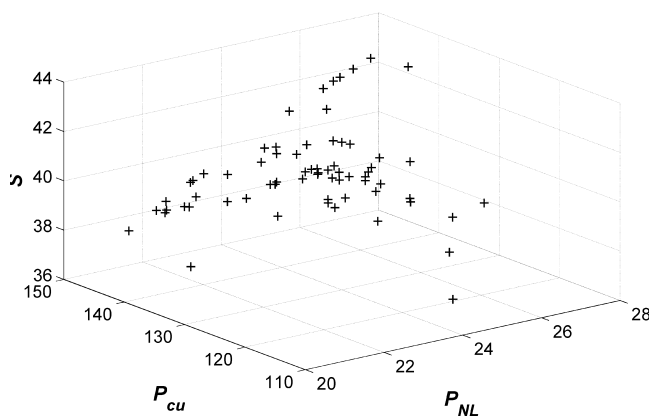


Fig. 3 Obtained Pareto front for the 40 MVA transformer.

**Table 1** Comparison between actual and computed design parameters and performance indicators for a 25 MVA transformer having  $K_W = 2.28$ .

25 MVA, $K_W = 2.28$		Actual values	Computed values
Main design parameters	$H_W$ (m)	1.37	1.50
	$J$ (kA/m <sup>2</sup> )	1.70	2.05
	$B$ (T)	1.61	1.63
	$D$ (m)	0.54	0.56
Performance indicators	$S$ (MVA)	25	25.11
	$P_{cu}$ (kW)	85.20	85.00
	$P_{NL}$ (kW)	15.50	15.22
	$X\%$	10.48	10.45
Cost indicators	Core volume (m <sup>3</sup> )	2.10	2.30
	Copper volume (m <sup>3</sup> )	1.14	0.80

**Table 2** Comparison between actual and computed design parameters and performance indicators for a 40 MVA transformer having  $K_W = 2.05$ .

40 MVA, $K_W = 2.05$		Actual values	Computed values
Main design parameters	$H_W$ (m)	1.37	1.37
	$J$ (kA/m <sup>2</sup> )	2.17	2.58
	$B$ (T)	1.75	1.74
	$D$ (m)	0.61	0.64
Performance indicators	$S$ (MVA)	40.00	40.24
	$P_{cu}$ (kW)	135.90	135.98
	$P_{NL}$ (kW)	24.70	24.17
	$X\%$	11.00	11.01
Cost indicators	Core volume (m <sup>3</sup> )	2.67	2.98
	Copper volume (m <sup>3</sup> )	1.02	0.81

volt-ampere rating and power loss requirements. In the first computation set, design parameters corresponding to 30 MVA and 50 MVA transformer ratings having the same specifics, per-unit reactances and percentage total copper and no-load losses (i.e., efficiencies) were computed. Expectedly, as shown in Fig. 4, almost all design parameter values increase

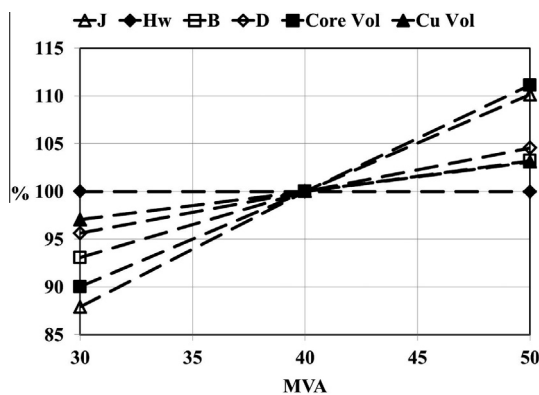


Fig. 4 Variation of the design parameters for different transformer ratings having the same specifics, per-unit reactances and total copper and no-load loss percentages.

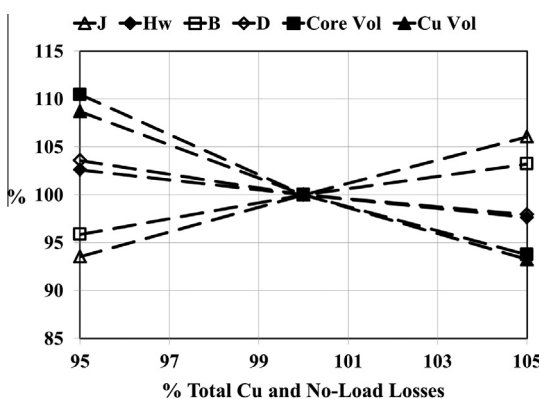


Fig. 5 Variation of the design parameters for 40 MVA transformers having the same specifics, per-unit reactances for different total copper and no-load loss percentages (i.e., efficiencies).

as the transformer rating is increased while maintaining the same percentage total copper and no-load losses. It should be mentioned here that  $H_W$  variation is minimal in these cases since transformer voltages are assumed unchanged. This suggests that any rating variation will similarly affect the phase currents squared and total copper loss values, thus minimally affecting  $H_W$  as indicated by expression (14). In the second computation set, design parameters corresponding to 40 MVA transformer ratings having the same specifics, per-unit reactances but while varying the percentage total copper and no-load losses (i.e., efficiencies) are computed. As shown in Fig. 5, a smaller loss restriction is achieved by a larger size transformer with reduced current and flux density values. This is a particularly encountered design trade-off between capital and running costs for a power transformer.

**Conclusions**

In this paper, a performance-oriented power transformer design methodology using multi-objective evolutionary optimization has been introduced in detail. Experimental testing as well as other presented computational results clearly demonstrates the qualitative and quantitative accuracy of the

methodology. One advantage of using multi-objective evolutionary optimization is that it deals simultaneously with a set of possible solutions (i.e., a population). This enables finding several members of the Pareto front in a single run of the algorithm instead of having to perform a series of separate runs as in the case of classical optimization methods. These options can be extremely useful to minimize overall production costs in view of the changing global prices of different transformer components, especially copper and steel laminations.

The proposed methodology may be easily utilized to obtain a quick first guess design details for more sophisticated design approaches such as those utilizing FEA packages. Moreover, in the presence of detailed design strategies, the proposed methodology may be easily improved to relax some assumptions by including those strategies. Future work is planned to enhance the accuracy of the proposed methodology as well as to extend its applicability to cover more detailed transformer design aspects.

### Conflict of interest

*The authors have declared no conflict of interest.*

### Compliance with Ethics Requirements

*This article does not contain any studies with human or animal subjects.*

### References

- [1] Adly AA, Abd-El-Hafiz SK. Automated transformer design and core rewinding using neural networks. *J Eng Appl Sci* 1999;46:351–64.
- [2] Tsili MA, Kladas AG, Georgilakis PS, Souflaris AT, Paparigas DG. Advanced design methodology for single and dual voltage wound core power transformers based on a particular finite element model. *Electric Power Syst Res* 2006;76:729–41.
- [3] Tsili MA, Kladas AG, Georgilakis PS. Computer aided analysis and design of power transformers. *Comput Ind* 2008;59:338–50.
- [4] Georgilakis PS, Tsili MA, Souflaris AT. A heuristic solution to the transformer manufacturing cost optimization problem. *J Mater Process Technol* 2007;181:260–6.
- [5] Hernández C, Arjona MA. Design of distribution transformers based on a knowledge-based system and 2D finite elements. *Finite Elem Anal Des* 2007;43:659–65.
- [6] Georgilakis PS. Recursive genetic algorithm-finite element method technique for the solution of transformer manufacturing cost minimization problem. *IET Electr Power Appl* 2009;3:514–9.
- [7] Georgilakis PS, Olivares JC, Esparza-Gonzalez MS. An evolutionary computation solution to transformer design optimization problem. In: 7th International conference on electrical and electronics engineering research (CIIIEE), Aguascalientes, Mexico, November 10–12; 2010. p. 226–31.
- [8] Hernández C, Arjona MA. An intelligent assistant for designing distribution transformers. *Expert Syst Appl* 2008;34:1931–7.
- [9] Hengsi Q, Kimball JW, Venayagamoorthy GK. Particle swarm optimization of high-frequency transformer. In: 36th Annual conference on IEEE industrial electronics society (IECON), Glendale, AZ, USA November 7–10; 2010. p. 2914–9.
- [10] Rashtchi V, Bagheri A, Shabani A, Fazli S. A novel PSO-based technique for optimal design of protective current transformers. *Int J Comput Math Electric Electron Eng (COMPEL)* 2011;30:505–18.
- [11] Jalilvand A, Bagheri A. Optimal design of protective current transformer using PSO algorithm. In: International conference on intelligent and advanced systems (ICIAS), Kuala Lumpur, Malaysia, June 15–17; 2010. p. 1–5.
- [12] Du J, Feng Y, Wu G, Li P, Mo Z. Optimal design for rectifier transformer using improved PSO algorithm. In: International conference on measuring technology and mechatronics automation (ICMTMA), Changsha, China, March 13–14; 2010. p. 828–31.
- [13] Du J, Li P, Wu G, Bai H, Shen J. Improved PSO algorithm and its application in optimal design for rectifier transformer. In: International conference on intelligent computing and integrated systems (ICISS), Guilin, China, October 22–24; 2010. p. 605–8.
- [14] Chiandussi G, Codegone M, Ferrero S, Varesio FE. Comparison of multi-objective optimization methodologies for engineering applications. *Comput Math Appl* 2012;63:912–42.
- [15] Sawhney AK. A course in electrical machine design. Delhi: Dhanpat Rai & Sons; 1984.
- [16] Flanagan WM. Handbook of transformer design and applications. New York: McGraw Hill; 1992.
- [17] Kulkarni SV, Khaparde SA. Transformer engineering, design and practice. New York: Marcel Dekker, Inc.; 2004.
- [18] Saleh A, Adly A, Fawzi T, Omar A, El-Debeiky S. Estimation and minimization techniques of eddy current losses in transformer windings. In: Proceedings of the CIGRE conference, Paris, France, August; 2002. p. 1–6 [paper no. 12-105].
- [19] Saleh A, Omar A, Amin A, Adly A, Fawzi T, El-Debeiky S. Estimation and minimization techniques of transformer tank losses. In: Proceedings of the CIGRE conference, Paris, France, August; 2004. p. 1–6 [paper no. A2-104].
- [20] Adly AA, Abd-El-Hafiz SK. Utilizing particle swarm optimization in the field computation of nonlinear media subject to mechanical stress. *J Appl Phys* 2009;105:07D507.
- [21] Adly AA, Mayergoyz ID. Simulation of field-temperature effects in magnetic media using anisotropic Preisach models. *IEEE Trans Magn* 1998;34:1264–6.
- [22] Bui LT, Alam S. Multi-objective optimization in computational intelligence: theory and practice. IGI Global 2008 [chapter 2].
- [23] Kennedy J, Eberhart R. Particle swarm optimization. In: Proceedings of the IEEE int conf neural networks, Perth, Australia, November; 1995. p. 1942–8.
- [24] Adly AA, Abd-El-Hafiz SK. Using the particle swarm evolutionary approach in shape optimization and field analysis of devices involving nonlinear magnetic media. *IEEE Trans Magn* 2006;42:3150–2.
- [25] Adly AA, Abd-El-Hafiz SK. Speed range based optimization of non-linear electromagnetic braking systems. *IEEE Trans Magn* 2007;43:2606–8.
- [26] Adly AA, Abd-El-Hafiz SK. Utilizing particle swarm optimization in the field computation of non-linear magnetic media. *J Appl Comput Electromagnet Soc* 2003;18:202–9.
- [27] Adly AA, Abd-El-Hafiz SK. Field computation in non-linear magnetic media using particle swarm optimization. *J Magn Mater* 2004;272–276:690–2.
- [28] Tripathi PK, Bandyopadhyay S, Pal SK. Multi-objective particle swarm optimization with time variant inertia and acceleration coefficients. *Inf Sci* 2007;177:5033–49.
- [29] < [www.aksteel.com/markets\\_products/electrical.aspx#transformer](http://www.aksteel.com/markets_products/electrical.aspx#transformer) > .